



OTC 6062

## Computation of Nodule Abundance From Seabed Photos

by R. Sharma, Natl. Inst. of Oceanography

Copyright 1989, Offshore Technology Conference

This paper was presented at the 21st Annual OTC in Houston, Texas, May 1-4, 1989.

This paper was selected for presentation by the OTC Program Committee following review of information contained in an abstract submitted by the author(s). Contents of the paper, as presented, have not been reviewed by the Offshore Technology Conference and are subject to correction by the author(s). The material, as presented, does not necessarily reflect any position of the Offshore Technology Conference or its officers. Permission to copy is restricted to an abstract of not more than 300 words. Illustrations may not be copied. The abstract should contain conspicuous acknowledgment of where and by whom the paper is presented.

### ABSTRACT

Correlation between water depth, nodule coverage, abundance from seabed photos and grabs and the relative abundance has been studied in different seabed settings based upon thickness of 'sediment water interface boundary' (SWIB) layer and extent of nodule burial at different locations. Whereas, nodule coverage and abundance have an inverse relation with thickness of SWIB layer (due to nodule burial), there is a good correlation (0.75) between nodule abundance in photo and grab. Relationships between actual nodule population and variable burial under the associated sediments have been established and mathematical formulae worked out to compute nodule abundance from seabed photos in different environmental settings.

### INTRODUCTION

Nodules are known to be buried to varying extents under the uppermost uncompacted sediment on the seabed or the 'Sediment-Water Interface Boundary' (SWIB) layer (Cronan and Tooms, 1967; Sorem and others, 1979), leading to an underestimation of nodule abundance from seabed photos (Frazer and others, 1978; Bastein-Thiry, 1979; Anonymous, 1982). Studies on

comparison of nodule abundance from grabs and photos have emphasized the need for a correction factor to be applied to photo estimates to account for buried nodules (Fewkes and others, 1979; Felix, 1980). However, no single correction factor can be applied to all estimates (Felix, 1980), as the nodule burial also depends upon the varying thickness of SWIB layer at each location (Sharma, In press).

Several methods have been proposed for estimating nodule abundance from photos (Bastein-Thiry, 1979; Fewkes and others, 1979; Handa and Tsurusaki, 1981) and have attained an accuracy of 50-80 % with respect to actual nodule abundance. This study aims at quantifying the burial of nodules and thickness of SWIB layer in different seabed settings which can be used to estimate nodule abundance accurately, so as to make seabed photography an independent and reliable tool for nodule exploration.

### METHODS

Seabed photographs, at 285 locations, were taken, using cameras attached to freefall grabs, 1-1.5 m above the seabed. Nodule

References and illustrations at end of paper.

coverage (C) was estimated in percent by superimposing a graph sheet and counting the number of squares falling on nodules with respect to area of the photograph. Hence,

$$C = \frac{a_n}{a_p} \times 100 \quad \dots (1)$$

where  $a_n$  = area of nodules in the photograph

$a_p$  = area of the photograph.

Nodule diameter (D) was calculated using the scale factor (Sf) as

$$Sf = \frac{a_p}{a_s} \quad \dots (2)$$

where  $a_s$  = area photographed on the seabed.

Nodule abundance from photos ( $A_p$ ) was estimated in kg/sq.m. as per Handa and Tsurusaki (1981); as

$$A_p = 7.7 \times C \times D/100 \quad \dots (3)$$

The relative abundance (RA) was calculated as :

$$RA = \frac{A_p}{A_g} \times 100 \quad \dots (4)$$

where  $A_g$  = abundance in grab, which is estimated by dividing nodule recovery (kg) by area of grab (sq. m). Since RA is calculated to show the percentage of agreement between photo and grab abundance, it also indicates the burial ratio (BR) of nodules;

$$BR = 100 - RA \quad \dots (5)$$

Therefore, if  $RA=80\%$ , then  $BR=20\%$ . For this study, locations with nil abundance in both photos as well as grabs were not considered as it indicates that these locations have no nodules. Also, where  $A_g$  is nil or much smaller than  $A_p$  are not considered as it indicates a possible failure of the grab to collect all the nodules.

## RESULTS AND DISCUSSION

In order to arrive at correct estimates of nodule abundance from photos, consideration should be given to two important factors, viz:

- (a) thickness of SWIB layer which can vary upto 10 cm or more (Sorem and others, 1979);

- (b) extent of nodule burial which varies from 0 to 100%.

For this purpose, data from all locations has been classified in 2 separate groups based on following criteria :

- (i) Penetration of camera trigger weight to indicate thickness of the SWIB layer.
- (ii) Relative abundance values indicating the extent of nodule burial.

### A. Thickness of SWIB layer

The classes in this group are based upon thickness of upper soft sediment layer indicated by penetration of camera trigger weight such as nil, very less (25%), intermediate (50%), high (75%), complete (100%). For these classes, the maximum, minimum, mean and standard deviation (SD) as well as correlation matrix have been worked out for depth, nodule coverage, nodule abundance from photo and grab and RA (Table 1,2).

The mean nodule coverage increases (from 3 to 48%) with decrease in thickness of SWIB layer because more and more nodules tend to be exposed. The mean nodule abundance in photos and grabs also increases from 1 to 13 and 4 to 16 kg/sq.m., respectively, with decrease in thickness of SWIB layer, except in class 1. In class 1, there is no sediment cover (trigger weight shows no penetration at all) due to rock exposures and Fe-Mn encrustations at these locations which are photographed as massive outcrops on seabed but cannot be sampled. Hence, there is a very good correlation ( $> 0.8$ ) between coverage, abundance in photo and product of coverage and diameter of nodule, except in class 1 (0.059).

There is also a good correlation ( $> 0.67$ ) between nodule coverage and abundance in grab in class 2, 3, and 4 although the source of data for both is different. The correlation between the grab abundance and the product of coverage with diameter as well as the abundance from photo is also slightly higher ( $> 0.68$ ) for all

classes, except for class 5 (0.53) in which many nodules are recovered in grabs, but not seen in photos due to very thick sediment cover (penetration 100%).

In areas of higher SWIB thickness, nodule distribution is more regular (SD is less) but areas of less penetration seem to have a patchy nodule distribution (SD is more). Depth, nodule coverage and abundance do not have a fixed range in any of the classes. Depth seems to have no control over thickness of SWIB layer or with any of the other parameters studied here.

#### B. Extent of nodule burial

Since, the extent of nodule burial is indicated by RA (%), the classes in this group are based upon different ranges of RA, such as 100-80%, 80-60%, 60-40%, 40-20%, 20-0%. The maximum, minimum, mean and standard deviation (SD) as well as correlation matrix for various parameters in this group have been worked out for all classes (Table 3, 4).

Mean nodule coverage and the nodule abundance in photo show a decreasing trend (from 27 to 1% and 8 to <1 kg/sq.m.) with increase in nodule burial. The mean nodule abundance in grab also decreases (from 11.14 to 4.6 kg/sq.m.) with increase in nodule burial (except for class 1a). The correlation between coverage, product of coverage with diameter, nodule abundance from photos and from grabs for all classes (except class 5e) is very high (> 0.87) and relatively less (0.7) for coverage and abundance from grab in case of all the data points. In class 5e, the nodule burial is > 80% so they are not recorded in photo, but collected in grab (hence very low correlation). Similarly, correlation between product of coverage with diameter, abundance from photos and grabs is less (0.69) for class 5e, as compared to correlation for classes 1a to 4d (> 0.94), whereas for all the data points it is 0.75.

The nodule distribution is very irregular in regions of less burial (SD is very high) as compared to areas with more buried nodules. There are no fixed

ranges for any parameter in different environmental settings except for relative abundance, since the classes in this group are based upon different RA (%) values. Depth has no relation with the extent of nodule burial as well as nodule coverage and abundance in the locations studied.

As observed in both the groups described above, the water depth has no control either over the thickness of SWIB layer and nodule burial or nodule coverage and abundance as the average water depth (~ 5100 m) does not vary substantially over the entire area. But, nodule coverage and abundance in photos and grabs have a significant (inverse) relation with SWIB thickness. Thicker the SWIB layer, more is the burial, so less nodules are seen in photos and collected in grabs. It is also possible that the buried nodules have no hydrogenous input of metals, so grabs recover less nodules as compared to areas with thin SWIB layer.

#### C. Relation between SWIB thickness, nodule burial and actual nodule abundance

In order to establish the relation between actual nodule abundance and extent of nodule burial (and SWIB thickness) at various locations, scatter diagrams were plotted for nodule abundance recorded in grab and photo parameters - nodule coverage and diameter for all the classes as well as all data points in each criteria.

#### Criteria I : Based on SWIB thickness

The plots taken for classes in this criteria have been shown in Fig. 1. Some classes have very few data points as locations belonging to those seabed conditions are very few in the area. For example, class 1 and 2 where there is nil or very less penetration are normally found on the summits of seamounts and abyssal hills which are not so common as other plain areas with more sediment thickness. The coefficient of regression is quite high (> 0.68) for all the classes as well as all data points

(0.75)', except for class 5, wherein sometimes all nodules are buried. The equation obtained (Table 5) does not vary substantially from one class to the other in this group.

#### Criteria 2 : Based on nodule burial

The plots taken for classes in this criteria have been shown in Fig. 2. Coefficient of regression is quite high ( $> 0.69$ ) for all classes as well as all data points in this group (0.75). The equation obtained (Table 5) shows a higher slope with increase in thickness of SWIB layer.

For estimation of nodule abundance from photos, both criteria can be employed depending upon the background information of the area. If the area has not been surveyed earlier, criteria 1 will prove more reliable as nodule abundance from photos can also be estimated by using the formula corresponding to the thickness of SWIB layer indicated by penetration of trigger weight and then compared with grab data, so they supplement each other.

Mathematical formulae in criteria 2, can be used during detailed surveys where the extent of nodule burial is known from previous surveys and results can be checked. This method can be used even while using deep-towed cameras without grab attachment. However, this method needs further confirmation.

In any area however, any of the mathematical relationships for all the data points can be safely used as they are more or less similar for both the criteria. Moreover, the slope of the line is similar to the one obtained by Handa and Tsurusaki (1981) in a part of the Pacific Ocean, but there is an addition of the constant factor in the formulae presented in the study which is an improvement over the earlier evolved equation.

#### CONCLUSIONS

The parameters studied from photos (coverage, diameter and photo abundance) are generally well correlated to the grab data and

sound relationships can be established between them. Depending upon seabed conditions, coverage and photo abundance may vary to different degrees with respect to actual nodule population, a knowledge of which can lead to establishing mathematical relationships, so as to use photos independently and reliably to estimate nodule abundance.

The major observations are :

- (1) Nodule abundance in photo and grab are generally well correlated except in areas of thick sediment cover, i.e. high nodule burial.
- (2) Although, average nodule coverage and abundance decrease with increase in thickness of SWIB layer, nodule population has no specific range of maximum and minimum values in different seabed settings (i.e. thickness of SWIB layer).
- (3) Water depth in nodule areas, does not seem to have any control over the thickness of SWIB layer or nodule burial, but they may be controlled by local topographic variations.

The computation of mathematical relationships between varying thickness of SWIB layer (or nodule burial) and nodule abundance offers an option to the user to use a general equation or a specific one depending upon the seabed conditions.

Thus seabed photography can be used effectively to demarcate areas for further surveys with other equipment. With knowledge of seabed conditions at different places more reliable data can be obtained using deep sea cameras which will be time saving as well as economical.

#### ACKNOWLEDGEMENTS

The author acknowledges constant support and encouragement from R.R. Nair, Asstt. Director, NIO. Author is grateful to V.N. Kodagali for developing software, Jaishankar for assistance in data processing, V.M. Date and H.D. Punj

for figures and slides and colleagues for discussions. This study was carried out with financial support from Department of Ocean Development, Govt. of India under the program "Surveys for polymetallic nodules".

#### REFERENCES

1. Cronan, D. S. and Tooms, J. S.: "Subsurface concentrations of manganese nodules in Pacific sediments". Deep Sea Research (1967) Vol. 14, 117-120.
2. Sorem, R. K., Fewkes, R. H., McFarland, W. B. and Reinhart, W. R. "Physical aspects of the growth environment in the Horn region, east equatorial Pacific Ocean". In : La Genese Des Nodules De Manganese, CNRS, Paris (1979), 61-76.
3. Frazer, J. Z., Fisk, M. B., Elliot, J., White, M. and Wilson, L. "Availability of copper, nickel, cobalt and manganese from ocean ferromanganese nodules". SIO report 78 -25. California, (1978), 138.
4. Bastein - Thiry, H. "Sampling and surveying techniques". In : Manganese nodules : Dimensions and Perspectives, UNOET, D. Reidel, Holland (1979), 7-20.
5. Anonymous. "Reliability of data parameters". In: Assessment of manganese nodule resources, UNOET, Graham and Trotman, London (1982), 15-30.
6. Fewkes, R. H., McFarland, W. D., Reinhart, W. R. and Sorem, R. K. "Development of a reliable method for evaluation of deepsea manganese nodule deposits". USBM report No. 64-80. NTIS, Virginia (1979), 91.
7. Felix, D. "Some problems in making nodule abundance estimates from sea floor photographs". Marine Mining, Vol.2 no. 3, (1980), 293-302.
8. Handa, K., Tsurusaki, K. "Manganese nodules : relationship between coverage and abundance in the northern part of Central Pacific Basin". In : GSJ Cruise report no. 15, ed. A. Mizuno, Japan (1981), 184-217.
9. Sharma, R. "Effect of sediment water interface boundary layer on exposure of nodules and their abundance". Jour. of Geol. Soc. of India., (In press).

TABLE 1  
 STATISTICAL PARAMETERS FOR CLASSES BASED  
 ON "SWIB" THICKNESS

Class	1	2	3	4	5
Penetration	Nil	25%	50%	75%	100%
No. of data	9	11	27	27	211
Depth Max.	5329	5637	5450	5725	5700
Min.	4560	4800	4815	4575	4575
Mean	4991	5245	5111	5096	5186
SD	273.9	220.6	170.6	184.6	177.8
Coverage Max.	95	70	75	40	65
Min.	1	9	0	0	0
Mean	48	39	25	15	3
SD	31.4	19	18	12	7.3
Abundance Max. (Photo)	14.43	21.56	16.17	11.78	14.62
Min.	0.0	2.00	0.0	0.0	0.0
Mean	2.23	12.60	7.1	4.49	1.02
SD	4.7	6.05	4.42	3.42	1.95
Abundance Max. (grab)	14.61	27.69	25.38	13.46	16.15
Min.	1.00	2.00	1.00	1.00	1.00
Mean	4.73	15.83	11.23	7.36	4.28
SD	4.53	6.44	5.14	3.44	4.07
RA (%) Max.	123.70	104.78	100.00	103.00	100.00
Min.	0.00	36.02	0.00	0.00	0.00
Mean	69.62	82.33	64.78	59.28	26.93
SD	48.30	21.71	33.23	33.42	41.44

TABLE 2

CORRELATION MATRICES FOR CLASSES BASED

ON "SWIB" THICKNESS

Class 1 : Trigger weight penetration = nil.

Depth	1.0000				
Coverage	0.3791	1.0000			
Abundance (ph)	-0.0071	0.0509	1.0000		
Abundance (gr)	-0.2443	0.1222	0.0316	1.0000	
Cov. x Diam.	-0.0060	0.0593	1.0000	0.0316	1.0000
Rel. Abundance	0.0073	-0.0052	0.4670	0.0230	0.4650
Depth	Cover.	Abun(Ph)	Abun(Gr)	C x D	RA

Class 4 : Trigger weight penetration = 75%.

Depth	1.0000				
Coverage	0.1300	1.0000			
Abundance (ph)	0.0026	0.9354	1.0000		
Abundance (gr)	0.0013	0.0727	0.7593	1.0000	
Cov. x Diam.	0.0500	0.9349	1.0000	0.7597	1.0000
Rel. Abundance	-0.0002	0.0700	0.0649	0.1205	0.0630
Depth	Cover.	Abun(Ph)	Abun(Gr)	C x D	RA

Class 2 : Trigger weight penetration = 25%.

Depth	1.0000				
Coverage	0.3900	1.0000			
Abundance (ph)	0.4534	0.9345	1.0000		
Abundance (gr)	0.1432	0.7628	0.0307	1.0000	
Cov. x Diam.	0.4533	0.9348	1.0000	0.0307	1.0000
Rel. Abundance	0.4705	0.3204	0.2009	-0.0013	0.2000
Depth	Cover.	Abun(Ph)	Abun(Gr)	C x D	RA

Class 5 : Trigger weight penetration = 100%.

Depth	1.0000				
Coverage	-0.1514	1.0000			
Abundance (ph)	-0.1000	0.0220	1.0000		
Abundance (gr)	-0.0702	0.4000	0.5320	1.0000	
Cov. x Diam.	-0.1010	0.9216	1.0000	0.5326	1.0000
Rel. Abundance	-0.0059	0.4526	0.5102	-0.0702	0.5102
Depth	Cover.	Abun(Ph)	Abun(Gr)	C x D	RA

Class 3 : Trigger weight penetration = 50%.

Depth	1.0000				
Coverage	0.5057	1.0000			
Abundance (ph)	0.4316	0.0217	1.0000		
Abundance (gr)	0.3213	0.7373	0.0035	1.0000	
Cov. x Diam.	0.4300	0.0215	1.0000	0.0035	1.0000
Rel. Abundance	0.2000	0.4074	0.0260	-0.0000	0.0260
Depth	Cover.	Abun(Ph)	Abun(Gr)	C x D	RA

All Classes

Depth	1.0000				
Coverage	-0.0072	1.0000			
Abundance (ph)	-0.0673	0.0000	1.0000		
Abundance (gr)	-0.0507	0.5970	0.7510	1.0000	
Cov. x Diam.	-0.0673	0.0000	1.0000	0.7516	1.0000
Rel. Abundance	-0.0004	0.4070	0.5505	0.1571	0.5503
Depth	Cover.	Abun(Ph)	Abun(Gr)	C x D	RA

TABLE 3  
 STATISTICAL PARAMETERS FOR CLASSES BASED  
 ON NODULE BURIAL

Class	1a	2b	3c	4d	5e
RA (%)	100-80	80-60	60-40	40-20	20-00
No. of data	29	22	28	43	147
Depth					
Max.	5637	5400	5725	5500	5550
Min.	4180	5000	4815	4614	4670
Mean	5104	5136	5126	5103	5220
SD	258.4	131.5	171.0	204.3	168.4
Coverage					
Max.	75	70	75	26	78
Min.	1	1	1	1	0
Mean	27	25	13	5	1
SD	19.5	17.8	15.4	6.2	6.6
Abundance (Photo)					
Max.	16.32	21.56	14.34	6.20	2.10
Min.	1.00	1.00	1.00	1.00	0.00
Mean	8.07	7.95	3.85	1.88	0.30
SD	5.10	4.70	3.30	1.50	0.51
Abundance (grab)					
Max.	19.61	27.69	25.38	18.46	15.30
Min.	1.00	1.50	1.69	2.76	1.00
Mean	8.77	11.14	7.33	6.52	4.60
SD	5.57	6.26	5.90	4.42	4.03
RA (%)					
Max.	100.00	79.57	59.17	39.23	20.00
Min.	81.26	61.32	40.65	20.32	00.00
Mean	91.37	70.48	51.49	28.40	3.40
SD	6.04	5.60	5.61	6.23	6.02



TABLE 4

CORRELATION MATRICES FOR CLASSES BASED ON NODULE BURIAL

<u>Class 1a</u> $\bar{1}$ $RA = 100-00\%$		<u>Class 4d</u> $\bar{1}$ $RA = 40-20\%$	
Depth	1.0000	Depth	1.0000
Coverage	0.3698 1.0000	Coverage	0.0280 1.0000
Abundance (ph)	0.4588 0.9281 1.0000	Abundance (ph)	0.0199 0.9731 1.0000
Abundance (gr)	0.4568 0.8972 0.9912 1.0000	Abundance (gr)	0.0401 0.9040 0.9407 1.0000
Cov. x Diam.	0.4688 0.9286 0.9998 0.9911 1.0000	Cov. x Diam.	0.0165 0.9731 0.9998 0.9471 1.0000
Rel. Abundance	0.1346 0.3127 0.2062 0.8947 0.2083 1.0000	Rel. Abundance	-0.0368 0.4019 0.3625 0.1007 0.3629 1.0000
Depth	Cover. Abun(Ph) Abun(Gr) C x D RA	Depth	Cover. Abun(Ph) Abun(Gr) C x D RA
<u>Class 2b</u> $\bar{1}$ $RA = 80-60\%$		<u>Class 5d</u> $\bar{1}$ $RA = 20-00\%$	
Depth	1.0000	Depth	1.0000
Coverage	0.3082 1.0000	Coverage	-0.1718 1.0000
Abundance (ph)	0.2481 0.8732 1.0000	Abundance (ph)	-0.2278 0.1423 1.0000
Abundance (gr)	0.2664 0.8929 0.9884 1.0000	Abundance (gr)	-0.1758 0.1987 0.5060 1.0000
Cov. x Diam.	0.2384 0.8736 1.0000 0.9882 1.0000	Cov. x Diam.	-0.2284 0.1414 0.9999 0.6953 1.0000
Rel. Abundance	0.0273 0.2111 0.4277 0.3012 0.4284 1.0000	Rel. Abundance	-0.2188 0.1069 0.9356 0.5648 0.9369 1.0000
Depth	Cover. Abun(Ph) Abun(Gr) C x D RA	Depth	Cover. Abun(Ph) Abun(Gr) C x D RA
<u>Class 3c</u> $\bar{1}$ $RA = 60-40\%$		<u>All Classes</u>	
Depth	1.0000	Depth	1.0000
Coverage	0.2288 1.0000	Coverage	-0.0548 1.0000
Abundance (ph)	0.0824 0.9454 1.0000	Abundance (ph)	-0.0628 0.8987 1.0000
Abundance (gr)	0.0508 0.9244 0.9945 1.0000	Abundance (gr)	-0.0537 0.7014 0.7525 1.0000
Cov. x Diam.	0.8829 0.9455 1.0000 0.9942 1.0000	Cov. x Diam.	-0.0627 0.8988 1.0000 0.7526 1.0000
Rel. Abundance	0.2029 0.3257 0.3089 0.2387 0.3099 1.0000	Rel. Abundance	-0.2385 0.6655 0.7767 0.4270 0.7762 1.0000
Depth	Cover. Abun(Ph) Abun(Gr) C x D RA	Depth	Cover. Abun(Ph) Abun(Gr) C x D RA

TABLE 5  
 FORMULAE FOR COMPUTING NODULE ABUNDANCE  
 IN DIFFERENT SEABED SETTINGS

---

Criteria 1 - Based on SWIB thickness:

Class	SWIB thickness	Trigger wt. penetration	Correlation coefficient	Relation to be used
1	Very thin	Nil	0.83	$Y = 6.18 X + 2.04$
2	Thin	Very less	0.83	$Y = 6.80 X + 4.62$
3	Intermediate	Intermediate	0.68	$Y = 5.90 X + 6.01$
4	Thick	High	0.76	$Y = 5.86 X + 3.93$
5	Very thick	Complete	0.53	$Y = 8.55 X + 3.14$
All	-	-	0.75	$Y = 7.54 X + 3.31$

---

Criteria 2 - Based on nodule burial:

Class	Nodule burial (†)	RA (†)	Correlation coefficient	Relation to be used
1a	00-20	100-80	0.99	$Y = 8.41 X - 0.01$
2b	20-40	80-60	0.98	$Y = 10.15 X + 0.67$
3c	40-60	60-40	0.99	$Y = 13.91 X + 0.37$
4d	60-80	40-20	0.95	$Y = 21.84 X + 1.20$
5e	80-100	20-00	0.69	$Y = 42.51 X + 2.97$
All	-	-	0.75	$Y = 7.74 X + 3.78$

---

$$X = C \times D / 100$$

C = Nodule coverage (†) in photo

D = Average nodule diameter in photo (cm)

Y = Abundance (Kg/sq.m)

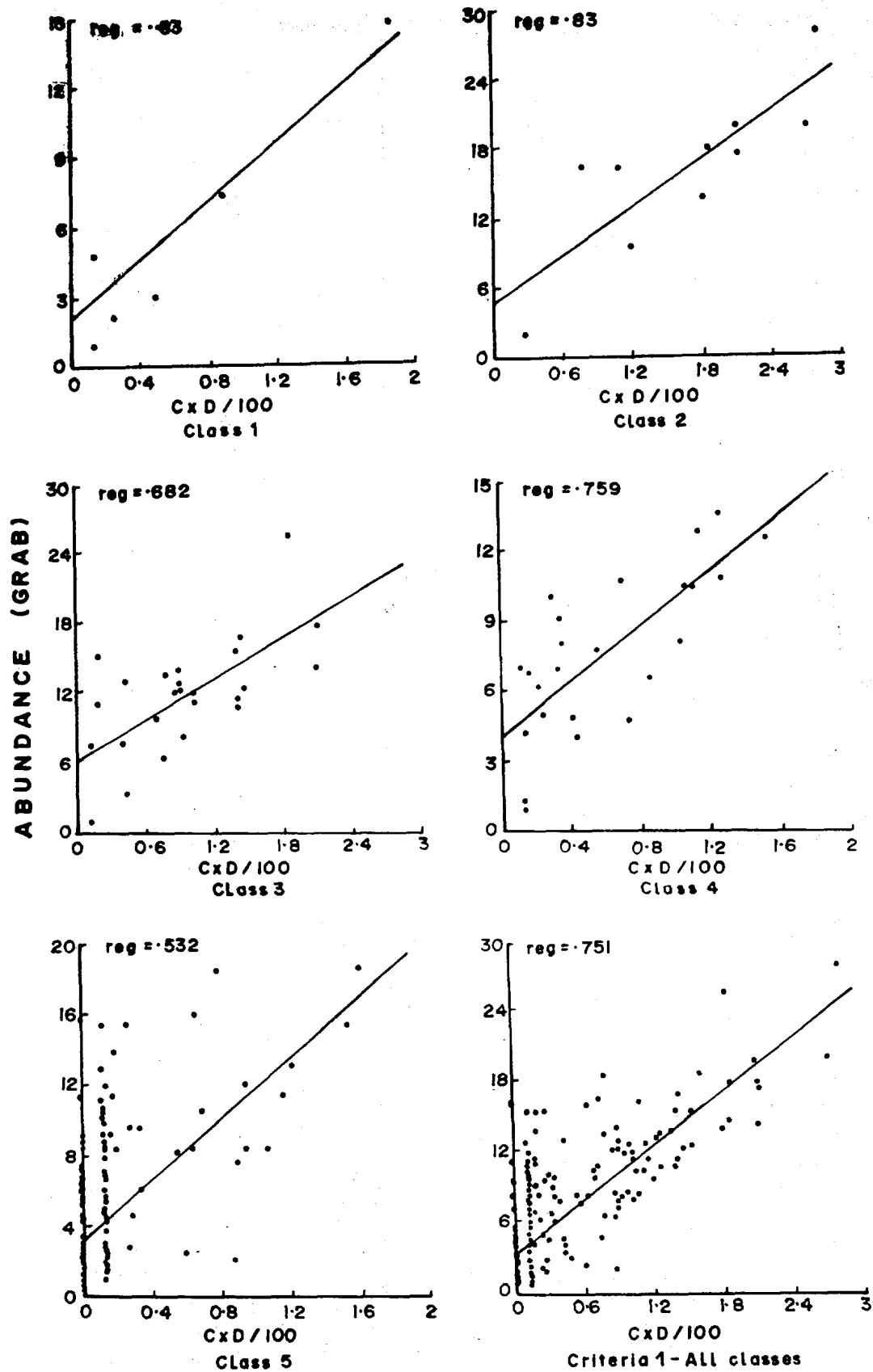


Fig. 1 Scatter diagrams for classes based on SWIB thickness

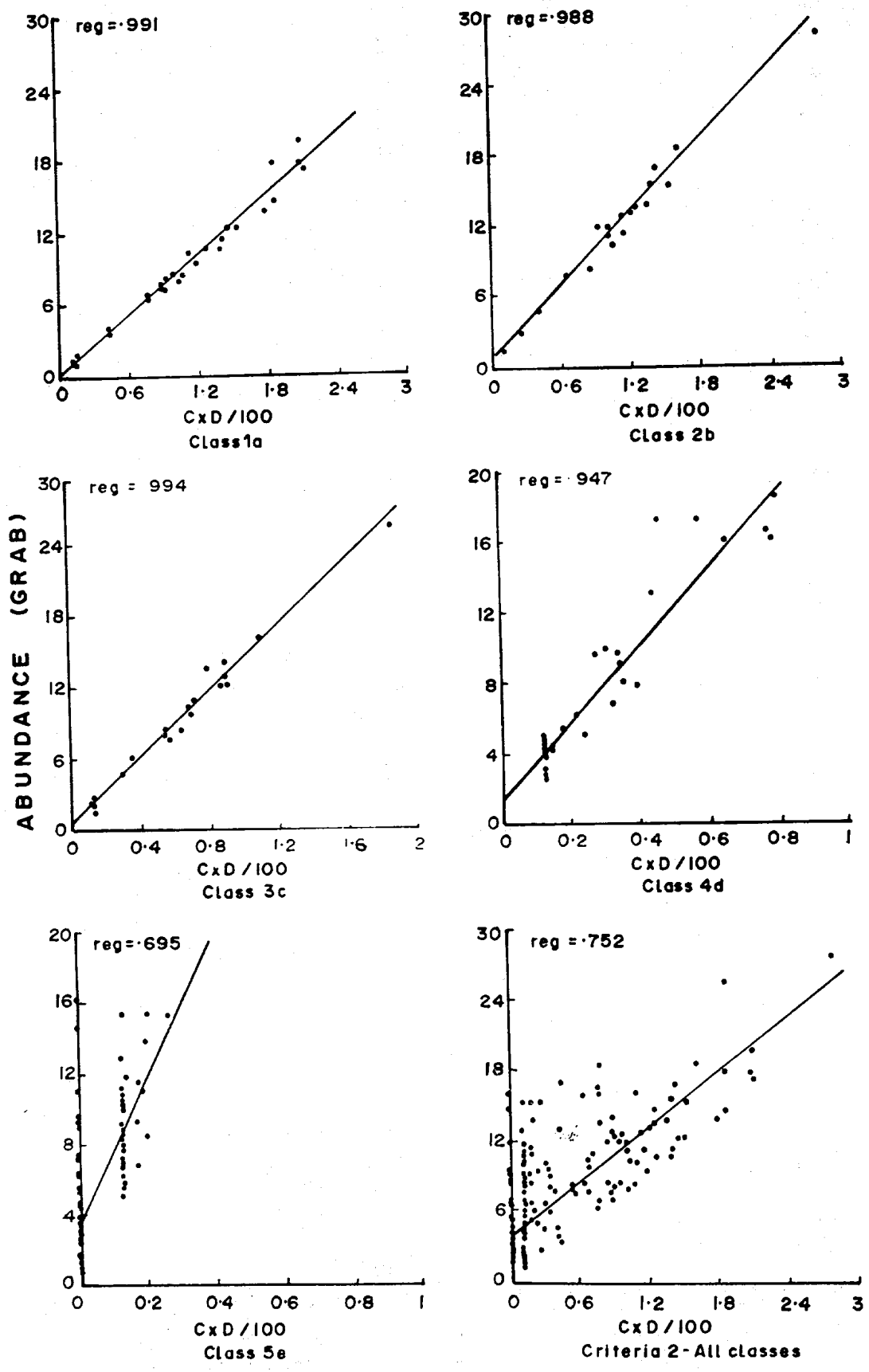


Fig. 2 Scatter diagrams for classes based on nodule burial